A Journal of the Gesellschaft Deutscher Chemiker

Angewandte International Edition

GDCh

Chemie

www.angewandte.org

Accepted Article

Title: 2D Oligosilyl Metal-Organic Frameworks as Multi-State Switchable Materials

Authors: David A. Burns, Eric M. Press, Maxime A. Siegler, Rebekka S. Klausen, and V. Sara Thoi

To be cited as: *Angew. Chem. Int. Ed.* 10.1002/anie.201912911
Angew. Chem. 10.1002/ange.201912911

Link to VoR: http://dx.doi.org/10.1002/anie.201912911
http://dx.doi.org/10.1002/ange.201912911

WILEY-VCH

10.1002/anie.201912911

WILEY-VCH

COMMUNICATION

2D Oligosilyl Metal-Organic Frameworks as Multi-State Switchable Materials

David A. Burns,[a] Eric M. Press,[a] M. A . Siegler,[a] and Rebekka S. Klausen,[a] V. Sara Thoi *[a]

Abstract: We report the synthesis of a set of 2D metal-organic frameworks (MOFs) constructed with organosilicon-based linkers. These oligosilyl MOFs feature linear $Si_nMe_{2n}(C_6H_4CO_2H)_2$ ligands (lin-Si_n, n = 2, 4) connected by Cu paddlewheels. The stacking arrangement of the 2D sheets is dictated by van der Waals interactions and is tunable by solvent exchange, leading to reversible structural transformations between many crystalline and amorphous phases.

Materials with states that are reversibly switchable upon exposure to external stimuli are powerful tools for a variety of applications such as sensing, memory storage, and electronic devices. Owing to their chemical and structural tunability, metal-organic frameworks (MOFs)—a class of highly porous materials composed of metal ions/clusters connected by organic linkers in two- or three-dimensional networks—have galvanized intense research efforts in the area of switchable materials.[1,2] Judicious choices of the metal and organic precursors have led to bistable MOF materials with magnetic,[3,4] electrical,[5] and optical states.[3] For instance, MOFs comprised of dithienylethene linkers undergo optically-induced structural transformations that change the properties of the pores for enhanced chemical separations.[6]

Recently, MOFs with stable amorphous and crystalline states have attracted attention as switchable materials.[7] Introduction of methanol or ethanol to a Co-based MOF led to reversible crystal-to-amorphous conversion and the emergence of new optical properties.[8] Another crystalline MOF, $Cu[Cu(pdt)_2]$, can be amorphized by heating at 120°C and returned to its crystalline state by soaking in acetonitrile.[9] The MOF was shown to have enhanced electronic conductivity in its amorphous state. Reversible crystalline-to-amorphous transformations have also been observed in proton-conducting lanthanide MOFs.[10] While bistable MOFs have created exciting opportunities for binary "on-off" applications, materials with multiple switchable states can offer multidimensionality for more complex functions (e.g. quantum computing).

In this work, we present two examples of MOFs capable of reversible structural transformations between multiple crystalline or amorphous phases. Oligosilanes, molecules with Si-Si bonds, are a class of hybrid inorganic-organic materials with remarkable light absorption and charge transport properties[11–16] that uniquely

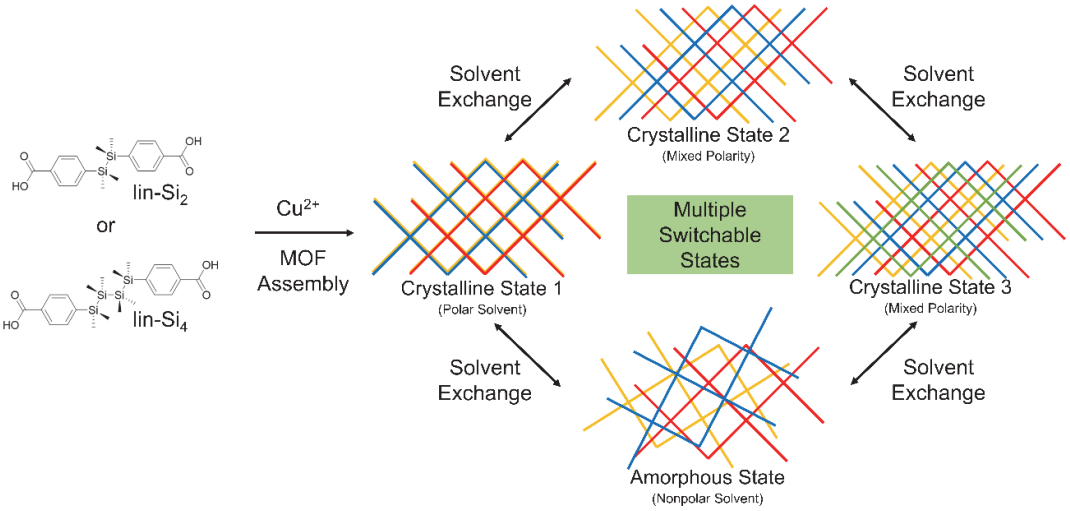

Scheme 1. Cu(lin-Si_n) MOFs are comprised of 2D sheets with solvent-dependent stacking arrangements. The interconversion of multiple states intimates potential applications for switchable materials.

[a] D. A. Burns, Dr. E. M. Press, Dr. M. A. Siegler, Prof. Dr. R. S. Klausen, Prof. Dr. V. S. Thoi*
Department of Chemistry
Johns Hopkins University
3400 N Charles Street
Baltimore, MD, 21218:
U.S.A.
Email: sarathoi@jhu.edu

Supporting information for this article is given via a link at the end of the document.

10.1002/anie.201912911

WILEY-VCH

COMMUNICATION

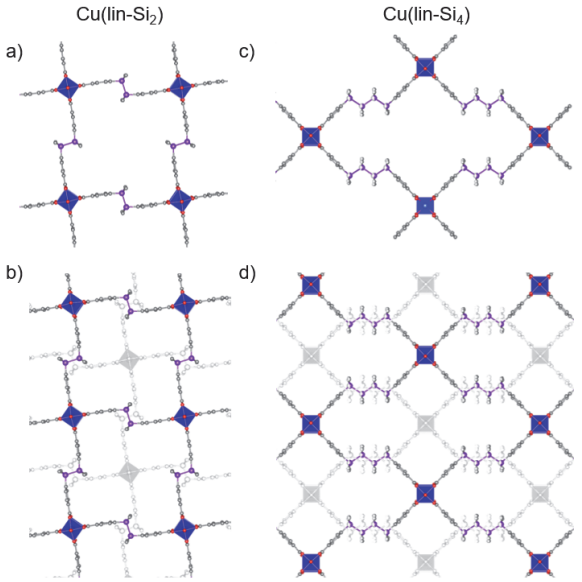

Figure 1. Monolayer segments and view of sheet stacking as seen down the stacking direction for Cu(lin-Si_2) (a, b) and Cu(lin-Si_4) (c, d). Key: Cu (blue polyhedra), Si (purple), C (grey), O (red); Hydrogens omitted for clarity. Greyscale indicates an underlying MOF sheet.

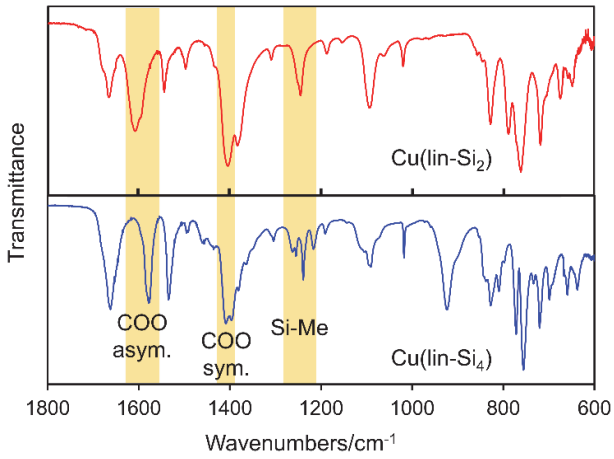

Figure 2. IR spectra of Cu(lin-Si_2) (top) and Cu(lin-Si_4) (bottom). Important spectral features are highlighted.

combine flexibility and strong light absorption, a property that inspired us to construct 2D MOFs based on oligosilyl linkers. While organosilicon species have been previously used in MOF formation,[17–20] the organic linker usually contains a single Si atom, which precludes access to properties inherent to σ-conjugated extended oligosilanes.

We report the first set of many possibilities for oligosilyl MOFs. The MOFs consist of Cu paddlewheel nodes connected by linear permethylated silicon chains, $Si_nMe_{2n}(C_6H_4CO_2H)_2$ (lin-Si_n, n = 2, 4) into a two-dimensional network. Scheme 1 illustrates the assembly of the Cu^{2+} ions and linkers into a layered 2D structure which is then transformed upon solvent exchange. We demonstrate structural control over the arrangement of the 2D sheets using simple solvent exchanges and heat treatment. As 2D MOFs are increasingly attractive materials for a range of applications due to their processability and layer control,[21–25] oligosilyl MOFs are well-positioned as a structurally tunable materials for a range of applications from sensing and molecular entrapment to optical and electronic applications.

Under solvothermal conditions, combining copper (II) salts with lin-Si_2 and lin-Si_4 yielded dark blue single crystals. Single Crystal X-Ray Diffraction revealed the Cu(lin-Si_n) MOFs share similar structural motifs (Figure 1). Each MOF is composed of water-bound Cu paddlewheel nodes connected in a network of two-dimensional sheets which are staggered in an AB fashion. Pore apertures of Cu(lin-Si_2) are roughly square-shaped with a width of 17.9 Å, while Cu(lin-Si_4) apertures are oblong with the widest width being 36.3 Å. The crystal morphologies of both MOFs closely mirror the structural motifs observed on the molecular level: Cu(lin-Si_2) and Cu(lin-Si_4) crystals have rectangular and “eye-shaped” morphologies, respectively. The stacking of MOF sheets appears to be driven by van der Waals interactions, as the only point of contact between 2D layers is at the oligosilyl portions of the linkers which align on top of one another. This arrangement of the methylated silicon chains in the MOFs gives rise to hydrophobic channels in the through-plane direction, especially in Cu(lin-Si_4). The silyl linkers in both cases are also in virtually perfect anti-conformations,[26] with dihedral angles along Si-Si bonds of 180° for lin-Si_2 and 179.4° in lin-Si_4. These dihedral angles suggest the MOF structures hold the oligosilyl linkers in the conformations most conducive to delocalization of electrons across the entire length of each linker.[11,27,28]

Altering the synthesis conditions yielded blue-green polycrystalline powder precipitates of Cu(lin-Si_n). Infrared spectroscopy (IR) confirms the presence of the silicon backbone (Figure 2). A single peak at 1246 cm^{-1} is observed in Cu(lin-Si_2), consistent with the Si-CH_3 stretch.[29] For Cu(lin-Si_4), a number of Si-CH_3 peaks are observed in the range of 1230-1260 cm^{-1}. In addition, peaks associated with the carboxylic acid groups of the protonated (unbound) linkers at 1682 cm^{-1}, 1423 cm^{-1}, and 1295 cm^{-1} are noticeably absent (Figure S9).[30] The difference in wavenumbers between the symmetric and asymmetric COO stretches falls within the range of 130-200 cm^{-1} for both materials, which confirms binding of carboxyl groups to two metal atoms as expected in the paddlewheel geometry.[31] Thus, the coordination environment in Cu(lin-Si_n) is retained in the polycrystalline powder form.

The 2D nature of these materials allows them to exhibit dynamic structural conversion between different stacking arrangements. These structural rearrangements can be reversibly tuned by solvent exchange, leading to multiple switchable crystalline states. Figure 3a shows the calculated Powder X-Ray Diffraction (PXRD) pattern for the Cu(lin-Si_2) crystals, which were formed in a highly polar solvent mixture of 1:3 H_2O/diethylformamide (DEF). Exposure of the MOF to a less polar solvent by washing with neat dimethylformamide (DMF), N-methyl-2-pyrrolidinone (NMP), or a mixture of dichloromethane (DCM) and acetone yielded crystalline materials with different diffraction patterns. The new PXRD patterns shift progressively to lower 2θ, with the most drastic structural changes being seen

10.1002/anie.201912911

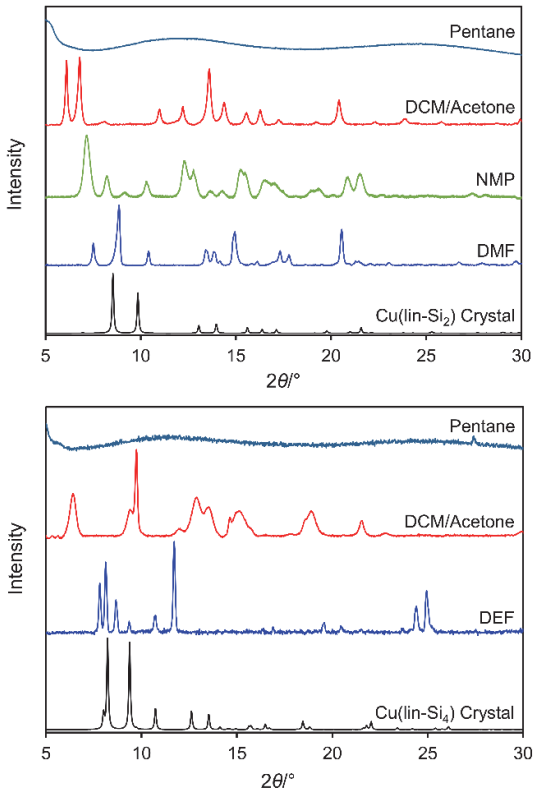

Figure 3. PXRD patterns for a) Cu(lin-Si_2) and b) Cu(lin-Si_4) in environments of reducing polarity from bottom to top. Background is subtracted for all scans except those denoted for pentane.

when the powder is exposed to DCM/acetone mixtures. Notably, each of these crystalline phases are interconvertible. Clear color changes in various shades of blue are also observed upon solvent exchange, suggesting that the Cu coordination environment is affected by the new solvents.[32] Structural refinement of the MOF powders was not possible due to the low intensities of the high-angle peaks; however, our results demonstrate that Cu(lin-Si_n) structures are highly sensitive to solvent inclusion.

These structural transformations of Cu(lin-Si_n) are interconvertible even from an amorphous powder, adding yet another accessible state. The long-range order of the MOFs is lost when the encapsulated solvent is either exchanged with pentane or removed altogether under heat and vacuum (Figure 3). However, just as the previous crystalline phases are interconvertible, crystallinity can be quickly restored to the amorphous MOF upon briefly soaking for a few hours in a polar solvent, as observed by PXRD (Figure 4). Furthermore, the IR spectra of air-dried MOF powders after exposure to different solvents confirm that the chemical connectivity is retained after each transformation (Figure S10). Similar solvent-dependent structural conversions are observed in the larger Cu(lin-Si_4) framework (Figure 3b).

We reason that the deviation from the high symmetry, tetragonal space group in the presence of different solvents is due to shifts in the 2D sheets of Cu(lin-Si_n) relative to one another. As the solvent molecules are introduced to the interlayer, the van der Waals forces, which dictate the arrangement of the 2D sheets, are disrupted and the structure is unable to accommodate a perfectly staggered, AB arrangement. We qualitatively observe how sliding one layer by 0.05 unit in the a and b direction can affect the diffraction pattern using the DIFFaX program.[33] We first modeled a series of perfectly staggered sheets of Cu(lin-Si_2) and demonstrated that DIFFaX pattern matches the calculated PXRD from the solid-state structure (Figure S11). After laterally translating each layer by ¼ of the unit cell in both *a* and *b* directions relative to the previous neighboring layer, the calculated powder diffraction peaks shift to lower angles, similar to the observed PXRD trend for Cu(lin-Si_2) MOF after being soaked in DCM/acetone. Our qualitative analysis demonstrates that solvent inclusion can lead to rearrangement of the 2D layers.

To explain the structural interconversion, we examined the chemical environment at the interlayer spacing. We hypothesize that there are two factors that direct the stacking arrangement of the 2D sheets: the polarity of the solvent system and the size of the ligand coordinated to Cu. The oligosilyl linkers are hydrophobic and can interact with one another. These hydrophobic interactions are maximized in the presence of polar solvents and can be observed in the crystal structures of Cu(lin-Si_n), where the vertical separation between Si-Me groups along the chains are a mere 1.67 Å and 1.83 Å (distance between the -CH_3 planes) for n = 2 and n = 4, respectively. The ability for the sheets to arrange in this AB fashion is also impacted by the identity of the coordinated molecule at the Cu centers. The small size of the coordinated H_2O allows the paddlewheels in the "A" sheets to be arranged directly above one another with a separation between the oxygen atoms of 5.746 Å for Cu(lin-Si_2) (Figure 5, left). In the case of Cu(lin-Si_4), this distance is slightly larger at 6.383 Å. The difference is likely due to slight wobbles observed in the crystal structure arising from the greater degrees of freedom in the longer oligosilane linkers. We note that the physical distance between the water molecules is even smaller when considering the O-H bonds, which are excluded from the figure for clarity.

Introduction of less polar and larger coordinating molecules creates new stacking arrangements. The reduced polarity of the solvent systems relieves the pressure upon the silicon chains to

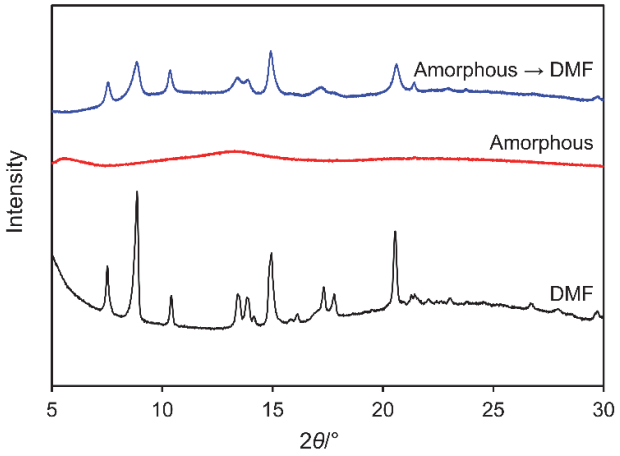

Figure 4. PXRD patterns of Cu(lin-Si_2) containing DMF (bottom), amorphous Cu(lin-Si_2) (middle), and the same amorphous Cu(lin-Si_2) with crystallinity quickly restored by immersing the MOF in DMF.

10.1002/anie.201912911

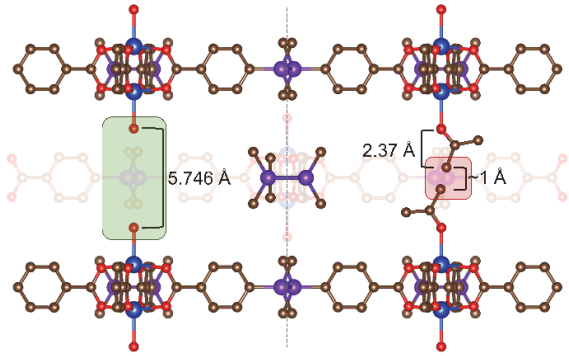

Figure 5. View of Cu(lin-Si_2) crystal structure looking down the *b* direction showing the vertical separation of an axially-bound H_2O (left) and acetone (to scale, right). The close proximity of the acetone suggests the structure must distort to accommodate larger coordinating ligands. Key: Cu (blue), Si (purple), C (brown), O (red); Hydrogens omitted for clarity. The transparency of the atoms indicate relative alignment; the oligosilyl components are directly alligned, likely through hydrophobic interactions.

maximize contact, while the larger coordinating ligands can displace the bound water and increase the interlayer spacing. Both of these effects contribute to deviations from the symmetric AB stacking and can cause the sheets to shift to minimize steric hindrances. To illustrate this point, we artificially introduced a coordinated acetone molecule to scale in the crystal structure of Cu(lin-Si_2) to examine the DCM/acetone solvent system. If all atomic positions in the structure are retained, there is only a ~1 Å separation between pendant carbon atoms of the two bound acetone molecules (Figure 5, right). Including the C-H bond lengths would further reduce the separation to well below the length of an average C-C bond. Steric repulsion would therefore necessitate a structural change to alleviate this stress. Simultaneously, the less polar DCM in the solvent system would help accommodate such a change by providing favorable interactions with the permethylated silicon chains. Extending our hypothesis to the most nonpolar solvent system in the pentane-exchanged MOFs, the purely nonpolar solvent environment enables the layers to rearrange with no single preferred orientation, resulting in an amorphous material.

Cu(lin-Si_n) are able to undergo further structural transformations under thermal activation. Thermogravimetric analysis demonstrates the thermal stability of Cu(lin-Si_2) in an argon atmosphere (Figure 6a). A mass loss event is observed at 205 °C, where Cu(lin-Si_2) undergoes loss of solvent (primarily DMF). Immediately following solvent removal, an exothermic peak in the heat flow curve is observed at 224 °C in a region where no mass is lost, which suggests desolvation triggers a physical phase change in the framework. Similar thermal behavior was observed for Cu(lin-Si_4) (Figure 6b); however, taking a closer look at the heat flow (Figure S12) reveals slight differences in behavior between Cu(lin-Si_2) and Cu(lin-Si_4). The Cu(lin-Si_2) event peaks at 224°C while the Cu(lin-Si_4) event peaks at 214 °C. The shoulder feature and broadness of the Cu(lin-Si_2) peak suggest a slower, multi-step process is occurring in contrast to the sudden, sharp transition in Cu(lin-Si_4). The more rapid transition in Cu(lin-Si_4) is also evidenced by the early onset of the Cu(lin-

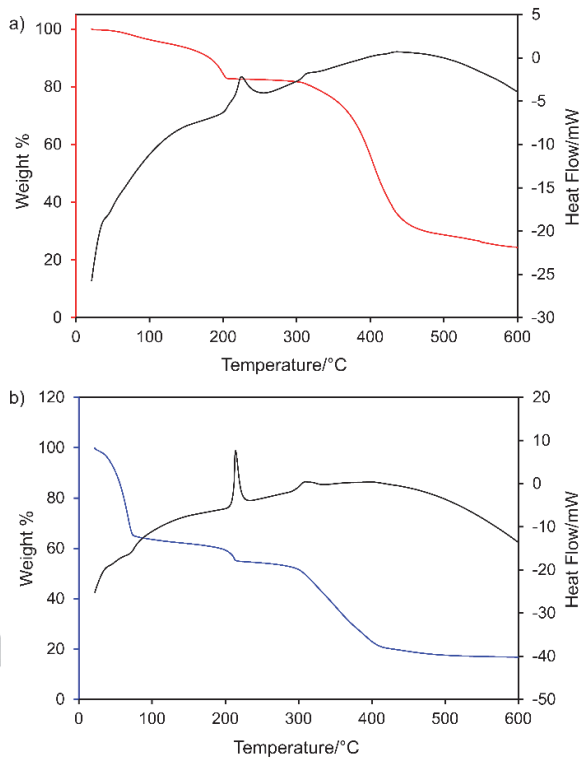

Figure 6. Percent weight loss and heat flow (mW) versus temperature curves for a) Cu(lin-Si_2) and b) Cu(lin-Si_4).

Si_4) heat flow peak at 207 °C just before the end of the mass loss which spans from 185-214 °C. Thus, the transition begins upon partial desolvation of the material. We expect that these differences arise from the larger aperture size in Cu(lin-Si_4) which allows for faster release of guest molecules and prompt rearrangement. Integration of the heat flow peaks also determines the amount of energy released during the transitions. Cu(lin-Si_4) releases 481.9 J/g while Cu(lin-Si_2) releases slightly less at 464 J/g. We postulate that the phase transition of Cu(lin-Si_4) is more energetically facile due to the greater flexibility of the four-silicon chain, which allows the MOF to transition more quickly as well as reach a more stable configuration. The longer chain length could also provide Cu(lin-Si_4) more opportunities to engage in more stabilizing hydrophobic interactions, hence the more stable final state.

To further explore this thermal behavior, Cu(lin-Si_2) is desolvated via solvent exchange with DCM followed by heating under vacuum at 140 °C for 30 minutes to yield a green clay-like material. In the IR spectra of desolvated Cu(lin-Si_2) in Figure S13, a new asymmetric COO peak appears at 1572 cm^{-1}. A similar phenomenon has been observed upon heating the analogous CuBDC (and related paddlewheel MOFs) where the IR feature is attributed to a new asymmetric COO stretch.[34–36] In the case of CuBDC, the open axial metal sites associate with oxygen atoms in carboxyl groups of neighboring paddlewheels. The IR spectral changes for desolvated Cu(lin-Si_2) are consistent with reported results in CuBDC and suggest the presence of a similar bridging carboxyl group between adjacent Cu paddlewheels.[36] The thermally-activated Cu(lin-Si_2) is largely amorphous by PXRD,

which is consistent that the removal of the coordinating ligand leads to facile shifting of the individual sheets. The flexibility of the organosilicon linker may further disrupt crystalline packing in the absence of a directing solvent. Reintroduction of a coordinating polar solvent molecule restores the crystallinity, suggesting that ligand coordination and solvent polarity are important for ordering the MOF layers. These reversible conversions further confirm the structural integrity of each 2D sheet.

In summary, we have demonstrated the use of oligosilyl moieties to generate a new class of chemically-responsive MOFs composed of Cu paddlewheel nodes and $Si_nMe_{2n}(PhCO_2H)_2$ linkers. Uniquely, Cu(lin-Si_n) MOFs can achieve multiple crystalline and amorphous states, offering new opportunities beyond binary "on-off" applications. We postulate the identity and polarity of the encapsulated solvent directs the stacking arrangements of the 2D MOF layers. Structural characterization of the various crystalline and amorphous MOF phases is under active experimental and computational investigation. The high degree of reversibility with these structural changes and the availability of multiple stable states are attractive for molecular sensing (e.g. alcohols, nitroaromatics, etc.) and memory storage applications among others. The modularity and diversity of these MOFs pave the way for a unique class of hybrid oligosilyl materials which take advantage of the unique chemical properties of oligosilanes.

CCDC 1893669, 1893670, and 1893671 contain the supplementary crystallographic data for this paper. These data are provided free of charge by The Cambridge Crystallographic Data Centre.

Acknowledgements

We thank the Department of Chemistry and Johns Hopkins University for instrumentation support, graduate student support, and start-up funding. D.A.B also thanks the Department of Chemistry for a Harry and Cleio Research Fellowship. R.S.K. thanks the Alfred P. Sloan Foundation for a Sloan Research Fellowship. We would also like to thank Mr. Hector Vivanco and Prof. Tyrel McQueen for assistance with PXRD.

Keywords: Metal-Organic Frameworks • Silanes • 2D Materials • Structural Interconversion • Phase Change

[1] A. Schneemann, V. Bon, I. Schwedler, I. Senkovska, S. Kaskel, R. A. Fischer, *Chem. Soc. Rev.* **2014**, *43*, 6062–6096.

[2] Z. Chang, D.-H. Yang, J. Xu, T.-L. Hu, X.-H. Bu, *Adv. Mater.* **2015**, *27*, 5432–5441.

[3] M. Nihei, L. Han, H. Oshio, *J. Am. Chem. Soc.* **2007**, *129*, 5312–5313.

[4] E. Coronado, G. Mínguez Espallargas, *Chem. Soc. Rev.* **2013**, *42*, 1525–1539.

[5] R. A. Heintz, H. Zhao, X. Ouyang, G. Grandinetti, J. Cowen, K. R. Dunbar, *Inorg. Chem.* **1999**, *38*, 144–156.

[6] B. J. Furlong, M. J. Katz, *J. Am. Chem. Soc.* **2017**, *139*, 13280–13283.

[7] A. Halder, D. Ghoshal, *CrystEngComm* **2018**, *20*, 1322–1345.

[8] H. Tan, Q. Chen, Y. Sheng, X. Li, H. Liu, *CrystEngComm* **2018**, *20*, 6828–6833.

[9] J.-W. Xiu, G.-E. Wang, M.-S. Yao, C.-C. Yang, C.-H. Lin, G. Xu, *Chem. Commun.* **2017**, *53*, 2479–2482.

[10] R. M. P. Colodrero, K. E. Papathanasiou, N. Stavgianoudaki, P. Olivera-Pastor, E. R. Losilla, M. A. G. Aranda, L. León-Reina, J. Sanz, I. Sobrados, D. Choquesillo-Lazarte, et al., *Chem. Mater.* **2012**, *24*, 3780–3792.

[11] R. D. Miller, J. Michl, *Chem. Rev.* **1989**, *89*, 1359–1410.

[12] J. Koe, M. Fujiki, in *Organosilicon Compd.*, Elsevier, **2017**, pp. 219–300.

[13] R. S. Klausen, J. R. Widawsky, M. L. Steigerwald, L. Venkataraman, C. Nuckolls, *J. Am. Chem. Soc.* **2012**, *134*, 4541–4544.

[14] T. A. Su, H. Li, R. S. Klausen, N. T. Kim, M. Neupane, J. L. Leighton, M. L. Steigerwald, L. Venkataraman, C. Nuckolls, *Acc. Chem. Res.* **2017**, *50*, 1088–1095.

[15] J. Zhou, S. K. Surampudi, A. E. Bragg, R. S. Klausen, *Chem. - A Eur. J.* **2016**, *22*, 6204–6207.

[16] S. Surampudi, M.-L. Yeh, M. A. Siegler, J. F. M. Hardigree, T. A. Kasl, H. E. Katz, R. S. Klausen, *Chem. Sci.* **2015**, *6*, 1905–1909.

[17] J. B. Lambert, Z. Liu, C. Liu, *Organometallics* **2008**, *27*, 1464–1469.

[18] R. P. Davies, R. J. Less, P. D. Lickiss, K. Robertson, a J. P. White, *Inorg. Chem.* **2008**, *47*, 9958–9964.

[19] R. P. Davies, R. Less, P. D. Lickiss, K. Robertson, A. J. P. White, *Cryst. Growth Des.* **2010**, *10*, 4571–4581.

[20] I. Timokhin, J. Baguña Torres, A. J. P. White, P. D. Lickiss, C. Pettinari, R. P. Davies, *Dalt. Trans.* **2013**, *42*, 13806.

[21] M. Xu, S.-S. Yang, Z.-Y. Gu, *Chem. - A Eur. J.* **2018**, *24*, 15131–15142.

[22] W. Zhao, J. Peng, W. Wang, S. Liu, Q. Zhao, W. Huang, *Coord. Chem. Rev.* **2018**, *377*, 44–63.

[23] M. G. Campbell, D. Sheberla, S. F. Liu, T. M. Swager, M. Dincă, *Angew. Chemie Int. Ed.* **2015**, *54*, 4349–4352.

[24] K. Wada, K. Sakaushi, S. Sasaki, H. Nishihara, *Angew. Chemie Int. Ed.* **2018**, *57*, 8886–8890.

[25] J. Huang, Y. Li, R.-K. Huang, C.-T. He, L. Gong, Q. Hu, L. Wang, Y.-T. Xu, X.-Y. Tian, S.-Y. Liu, et al., *Angew. Chemie Int. Ed.* **2018**, *57*, 4632–4636.

[26] J. Michl, R. West, *Acc. Chem. Res.* **2000**, *33*, 821–823.

[27] J. C. Giordan, J. H. Moore, *J. Am. Chem. Soc.* **1983**, *105*, 6541–6544.

[28] H. Sakurai, M. Ichinose, M. Kira, T. G. Traylor, *Chem. Lett.* **1984**, *13*, 1383–1384.

[29] A. L. Smith, *Spectrochim. Acta* **1960**, *16*, 87–105.

[30] N. Koji, *Infrared Absorption Spectroscopy - Practical*, Holden-Day, San Francisco, California, **1964**.

[31] F. Verpoort, T. Haemers, P. Roose, J. P. Maes, *Appl. Spectrosc.* **1999**, *53*, 1528–1534.

10.1002/anie.201912911

[32] H. K. Kim, W. S. Yun, M.-B. Kim, J. Y. Kim, Y.-S. Bae, J. Lee, N. C. Jeong, *J. Am. Chem. Soc.* **2015**, *137*, 10009–10015.

[33] M. M. J. Treacy, J. M. Newsam, M. W. Deem, *Proc. R. Soc. A Math. Phys. Eng. Sci.* **1991**, *433*, 499–520.

[34] C. G. Carson, G. Brunnello, S. G. Lee, S. S. Jang, R. A. Gerhardt, R. Tannenbaum, *Eur. J. Inorg. Chem.* **2014**, *2014*, 2140–2145.

[35] L. N. McHugh, M. J. McPherson, L. J. McCormick, S. A. Morris, P. S. Wheatley, S. J. Teat, D. McKay, D. M. Dawson, C. E. F. Sansome, S. E. Ashbrook, et al., *Nat. Chem.* **2018**, *10*, 1096–1102.

[36] C. G. Carson, K. Hardcastle, J. Schwartz, X. Liu, C. Hoffmann, R. A. Gerhardt, R. Tannenbaum, *Eur. J. Inorg. Chem.* **2009**, *2009*, 2338–2343.

10.1002/anie.201912911

WILEY-VCH

Entry for the Table of Contents (Please choose one layout)

Layout 1:

COMMUNICATION

Going through a phase: Oligosilyl linker molecules were assembled into 2D metal-organic frameworks (MOFs) connected by copper paddlewheel nodes. Crystal structures demonstrate preferential anti-conformations of silicon chains. Powder X-ray diffraction reveals the crystalline phases of the MOFs are interconvertible through rearrangement of stacking motifs.

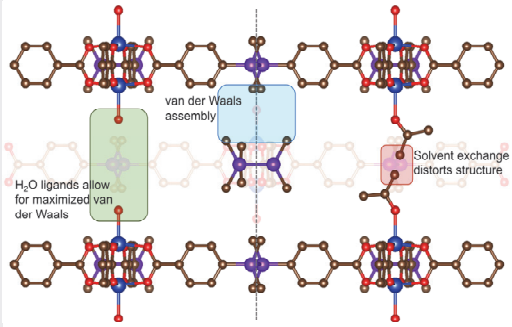

*David A. Burns, Eric M. Press, M. A. Siegler, and Rebekka S. Klausen, V. Sara Thoi **

Page No. – Page No.

2D Oligosilyl Metal-Organic Frameworks as Multi-State Switchable Materials

Layout 2:

COMMUNICATION

((Insert TOC Graphic here))

Text for Table of Contents

*Author(s), Corresponding Author(s)**

Page No. – Page No.

Title